ChemComm

Accepted Manuscript

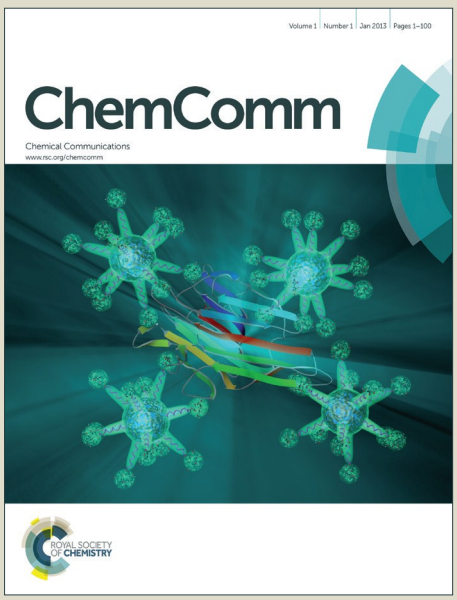

ROYAL SOCIETY OF CHEMISTRY

www.rsc.org/chemcomm

Cite this: DOI: 10.1039/c0xx00000x

www.rsc.org/xxxxxx

ARTICLE TYPE

Self-Assembly Pathway of Peptide Nanotubes Formed by a Glutamatic Acid-Based Bolaamphiphile

Emerson Rodrigo da Silva,*[a,b] Wendel Andrade Alves,[a] Valeria Castelletto,[b] Mehedi Reza,[c] Janne Ruokolainen,[c] Rohanah Hussain[d] and Ian William Hamley*[b]

Received (in XXX, XXX) Xth XXXXXXXXX 20XX, Accepted Xth XXXXXXXXX 20XX
DOI: 10.1039/b000000x

The self-assembly of peptide-nanotubes formed by an *L*-glutamic acid-based bolaamphiphile is shown to proceed via a remarkable mechanism where the peptide conformation changes from β-sheet to unordered. The kinetics of this process are elucidated via X-ray scattering and UV circular dichroism methods. The reverse transition from "unordered" to *β*-sheet structures is triggered by UV radiation.

Amphiphilic peptides have attracted much interest due to their remarkable ability to self-assemble into a large variety of nanoscopic polymorphs with impressive potential for designing soft materials applicable in biotechnology.[1] In most cases, these compounds mimic surfactant molecules with a single polar head of hydrophilic amino acids and a longer tail made from the association of nonpolar amino acids or the ester linkage of hydrocarbon chains. [1, 2] Interesting exceptions to this traditional single-headed layout are the so-called bolaamphiphiles, where a hydrophobic core appears flanked by two hydrophilic moieties at both ends of the chain.[3] This double-headed design gives rise to special properties and makes the description of aggregation phenomena in bolaamphiphiles more complex than in their single-headed counterparts.[4] In contrast to the extensive literature on the self-assembly of conventional amyloid peptides,[1, 5-9] work on bolaamphiphilic peptides is limited although a few studies involving *L*-glutamic acid terminated sequences have been reported in the last decade.[10-12] From this work, it has emerged that the chiral nature of *L*-glutamic acid head groups induces the formation of helical and tubular structures.[13] As a rule, however, these studies have focused on morphological aspects and used *ex-situ* techniques, mainly electron and atomic force microscopy, to reveal the organization of self-assemblies. A major drawback of such approaches is their inherent limitation in understanding the behaviour of these species in solution and in providing accurate information on the internal structure of the resulting polymorphs.

Here, we use small-angle X-ray scattering (SAXS) and synchrotron radiation circular dichroism (SRCD) to examine the structure and the self-assembly pathway of an amino acid-based bolaamphiphile, the linear octamer EFL_4FE (E = *L*-glutamic acid, F = *L*-phenylalanine and L = *L*-leucine). The hydrophobic region of the sequence is composed of four leucine repeats, an aliphatic amino acid often found in molecular zippers in protein aggregates.[14, 15] This aliphatic core is complemented by two phenylalanine moieties which are designed to assist lateral association due to π–π stacking interactions between aromatic rings.[16] The polar heads are made from *L*-glutamic acid moieties endowed with carboxyl groups. We found a remarkable and unexpected pathway of nanotube formation in which initial β-sheet structures are disrupted.

The EFL_4FE bolaamphiphile is not soluble in water at neutral pH, presumably due to the relatively low pKa (= 4.1) of its polar heads.[12] In this case, we dissolved the bolaamphiphile in 20 mM NaOH aqueous (or D_2O) solutions. The critical aggregation concentration (*cac*) has been measured through a pyrene fluorescence assay, as described elsewhere,[17] providing *cac* ~ 0.03 wt% (*ESI, Fig. S1*). EFL_4FE solutions were studied at concentrations above the *cac*, and left to equilibrate during a period between 10 and 12 days to ensure full self-assembly of the nanostructures. Cryo-TEM has been used to probe the change of self-assembled nanostructures.[18, 19] Representative Cryo-TEM images from 0.1 wt% EFL_4FE solutions (Fig. 1A) display flat membranes extending to a few hundred square nanometres (inset, Fig.1A). At higher concentration (1 wt% EFL_4FE, Fig. 1B) remarkable morphological changes appear and a large number of peptide nanotubes (PNTs) populate the sample. The high contrast between dark edges and bright cores indicates organization into hollow tubes, presumably made from scrolling of peptide sheets (inset, Fig.1B). The diameters of the tubes have been measured in the range 20 - 30 nm and their lengths have been found to easily reach the micrometre scale (*ESI, Fig.S2*).

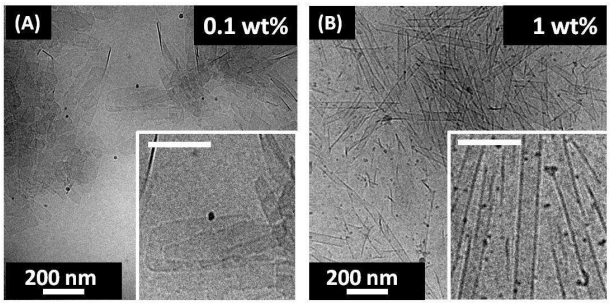

Fig. 1 Cryo-TEM micrographs showing self-assembly into well-defined flat sheets (A) or PNTs (B), depending on peptide concentration indicated in wt%. Insets scale bars: 100 nm.

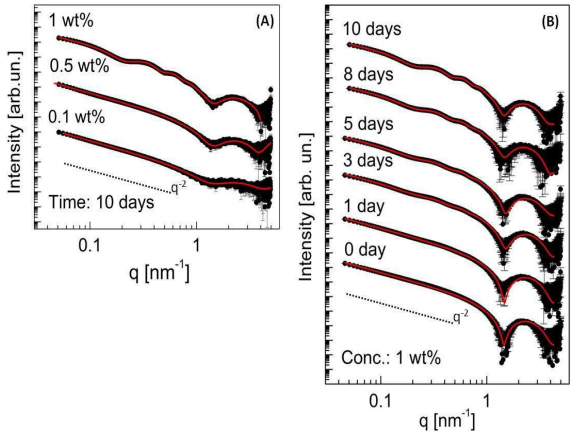

Fig. 2 SAXS data from solutions at the indicated incubation time and concentration. Red lines represent model fits using bilayer and cylindrical shell form factors as indicated in the text.

To get deeper structural information, we performed in situ synchrotron SAXS experiments. The SAXS curves in Fig.2A for solutions in the range (0.1- 1) wt% EFL_4FE show different features according to peptide concentration. For samples containing 0.1 and 0.5 wt% peptide, the curves are characterized by an initial intensity decay ~ q^{-2}, which is ascribed to the presence of flat nanostructures.[20] Data from these formulations have been fitted using the bilayer form factor proposed by Pabst *et al*.[21] Inspecting the parameters resulting from the best fits (*ESI, Table 1*), we observe that membrane thicknesses are ~ 3.3 nm, consistent with the molecular length of an octapeptide chain in a β-sheet conformation (8 × 0.34 nm = 2.72 nm)[22] plus monolayers of Na^+ ions partially buried into hydrophilic interfaces (Na^+ diameter ~ 0.37 nm).[23] Therefore, we conclude that EFL_4FE membranes are organized into monolayers where paired backbones appear oriented perpendicular to the outer surfaces. At 1 %wt EFL_4FE, SAXS shows oscillations in the low q region, highlighting a typical signature of tubular structures. To describe this domain, we have used a combination of the previous bilayer form factor plus a long cylindrical shell form factor (details in *ESI*).[20] The component associated to flat sheets reveals a thickness similar to that found in dilute samples, thus suggesting that peptide monolayers also appear in the mixture at higher concentration. Structural parameters associated to the cylindrical shell show the formation of nanotubes with average inner radius of 9.2 ± 1.6 nm, consistent with the sizes observed in cryo-TEM images. Interestingly, nanotube shells are found to be about 0.5 nm thicker than flat membranes, suggesting the wrapping into tubular geometry leads to stretching of peptide walls and/or a thicker counterion layer around the nanotubes.

We also prepared a second group of samples to investigate the time evolution of PNT formation. In this case, the concentration has been fixed at 1 wt% and solutions have been prepared over a period of days previous to SAXS experiments. In Fig. 2B, SAXS data from samples with aging times between 30 minutes and 10 days reveal remarkable differences upon aging. Data from fresh mixtures are fully described by the bilayer form factor, showing that organization into sheets is an early step in the self-assembly pathway. Also, the thicknesses of the resulting membranes are very close to those observed in dilute formulations, indicating ordering into monolayers (*ESI*, *Table1*). On the third day, however, oscillations at low q become more evident and a proper description of the data requires inclusion of the cylindrical shell form factor in the fit. The structural parameters (*ESI*, *Table1*) show that average nanotube radius decreases with time, ranging from 10.5 nm (day 3) to 9.6 nm (day 10). In addition, nanotube shells become slightly thicker upon incubation, increasing from 3.3 nm (day 3) to 3.8 nm (day 10). Observations performed on time scales longer than 10 days also revealed the signature of PNTs, with the same structural parameters derived above (*ESI, Fig. S4*).

The secondary structure has been probed using FTIR spectroscopy (*ESI, Fig. S5*). The amide *I* range is characterized by a sharp peak centred at 1620 cm^{-1} accompanied by a shallow broad band around 1685 cm^{-1}, indicating anti-parallel β-sheet conformation.[24, 25] Intense broad resonances around 1460 cm^{-1}, likely ascribed to scissoring modes of CH_2 groups in glutamic acid side-chains,[26] are not present in samples containing PNTs (*ESI, Fig. S5*). Anti-symmetric stretching vibrations of COO^- moieties[26] near 1565 cm^{-1} exhibit a strong decrease upon aging, possibly indicating neutralization of these species (*ESI, Fig. S6*). XRD measurements performed on dried stalks show that the crystal structure of the nanotubes is an orthorhombic unit cell with lattice parameters a = 31.15 Å, b = 11.17 Å and c = 9.82 (*ESI, Fig.S7 and table 2*). The amide-I region of the FTIR spectra (*ESI, Fig. S4*), measured for solutions containing only membranes, is similar to that measured for solutions containing mixtures of membranes with PNTs. However, a decrease in intensities of the characteristic FTIR bands upon increasing time, suggests a decrease of β-sheet content (*ESI, Fig. S6*).

CD data in the far-UV region allows more detail on the secondary structure of the self-assembled objects to be elucidated (*ESI, Fig. S8*). Dilute solutions, containing only membranes, exhibit features expected for β-rich structures with a strong maximum at 199 nm, traditionally ascribed to $\pi \rightarrow \pi^*$ transitions,[27] and a minimum at ~ 222 nm. In contrast with these β-sheet rich spectra, data from mixtures containing PNTs exhibit spectra dominated by an intense negative rotation at 199 nm and shallow maxima at 183, 208 and 217 nm (*ESI, Fig. S8*). These spectra, in shape and magnitude, resemble those associated to unordered structures,[28] with an additional contribution from the stacking of phenylalanine residues. The CD spectra show that the ordering of peptides in the nanotube walls is dominated by interactions between F residues rather than by the formation of of β-sheets.[29] The exact mechanisms leading to β-sheet-to-unordered transitions and subsequent formation of PNTs remain elusive; however, electrostatic repulsions between peptide chains and condensation of Na^+ onto glutamate units likely play a major role. The absence of wrapped structures in the dilute regime can be ascribed to the abundance of OH^- radicals competing for Na^+, which might hinder condensation of counter-ion layers. This process likely enables electrostatic repulsions between charged carboxylic groups, stabilizing a flat conformation. On the other hand, at higher concentrations, the buffering capacity is exhausted and OH^- radicals are consumed, enhancing condensation of Na^+. Indeed, the decrease of OH^- moieties is attested by a reduction of pH observed at high concentration. SAXS experiments in control samples dissolved in ethanol solutions (1:1 H2O:ETOH) indicated the formation of irregular aggregates, presumably

fractal structures, and no regular self-assemblies were observed after long time incubation. Also the secondary structure of these aggregates is dominated by β-sheet features (*ESI, Fig. S9*). Thus, the presence of additional counter-ions seems to be a necessary condition for the formation of PNTs. In addition, samples initially dissolved into NaOH which were further neutralized by addition of an equal amount of HCl exhibited the presence of nanosheets, but no PNTs were observed, even though the secondary structure shows some "unordered" aspects (*ESI, Fig. S10*). In this case, condensation of Na^+ is presumably prevented due to competition between Cl^- anions and glutamate units for cationic species.

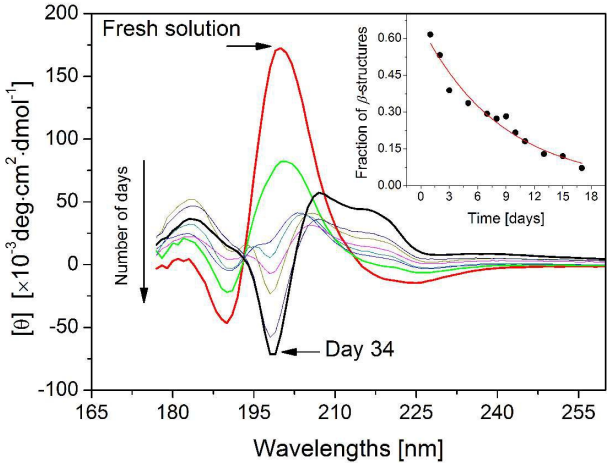

Fig. 3 CD spectra of EFL_4FE solutions monitored over a period of days. Inset: time-course of β-sheets fraction fitted by a simple exponential.

We also examined the time evolution of the secondary structure using CD. Spectra were measured for a 1 wt% solution over several days to correlate the formation of PNTs with the CD signature. In Fig. 3, we observe that conversion from β-sheet into unordered-like conformations takes a period of days. Fresh samples have been found to be dominated by β-sheets (red curve in Fig. 3), consistent with unfolded membranes indicated by SAXS results. The high sensitivity of CD technique reveals that unordered structures appear earlier than PNTs are detected in SAXS measurements. Indeed, a decrease of the intensity of the negative band at 199 nm is noticed after 1 day, suggesting bending of membranes already in the initial stages of aggregation (green curve in Fig. 3). To provide a more quantitative description of the time-course of the "β-to-unordered" transition, we have estimated the fraction of β-structures from the ellipticity at 199 nm (details in *ESI*). The time-course, inset in Fig. 3, is described by a simple exponential decay with characteristic time ~ 8.5 days, in agreement with increasing oscillations observed in SAXS data.

Solutions containing PNTs have been submitted to intense ultraviolet irradiation during synchrotron radiation circular dichroism (SRCD) experiments. In Fig. 4, we show a series of SRCD spectra from a series of measurements in the synchrotron beam. The major features of the scans are the changeover of the peculiar minimum at 199 nm into an intense maximum and two remarkable isochroic points at 191 and ~ 206 nm. In the first spectrum, the system is dominated by unordered conformations as expected for tubular assemblies. Nevertheless, upon successive irradiation, this conformation is gradually replaced by the characteristic profile of β-structures, indicating now an "unordered-to-β" transition. The fraction of β-structures has been calculated and the relationship between β-content and accumulated UV scans has been found to be well-described by a parabolic function (inset Fig. 4).

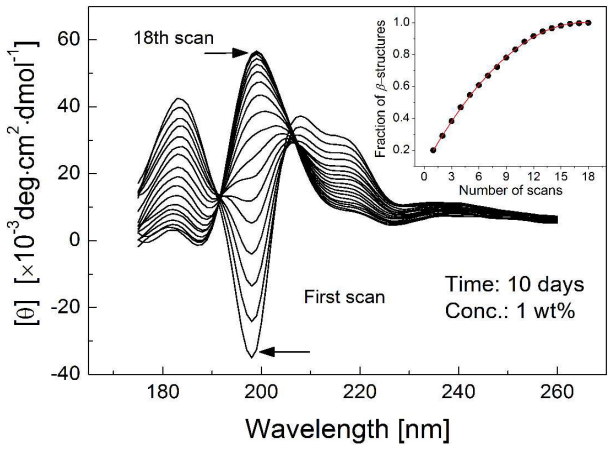

Fig. 4 Scan series of CD spectra showing changeover of unordered-like secondary structures into β-structures upon synchrotron ultraviolet irradiation. Inset: evolution of β-structures fraction fitted with a parabolic function.

To investigate if the origin of this transition could be associated to thermal effects introduced by the intense flux of synchrotron beamline, we conducted temperature-controlled assays using a lab CD machine (*ESI, Fig. S12*). Despite a decrease in the intensity of [θ] at 199 nm, we found that temperatures up to 90°C do not promote conversion into β-sheet structures; thus, disregarding the hypothesis that heating is responsible for the changeover shown in Fig. 4. In addition, thermal changes observed in the spectra have been found to be reversible upon cooling, a phenomenon not observed in samples exposed to intense UV-irradiation (*ESI, Fig. S13*). Putting these findings together, we hypothesize that the unordered to β-structure transition is due to photo-degradation induced by intense UV irradiation, possibly through oxidation of F side-chains.[30] This process likely changes the charge balance leading to destabilization of unordered architectures, followed by quick reorganization into β-sheet structures driven by strong hydrophobic interactions. Similar phenomena have been previously observed in X-ray triggered transitions in peptide filament networks.[31]

Summarizing, we have demonstrated the formation of PNTs by an exclusively amino acid-based bolaamphiphile in alkaline solution. The unique combination of high-resolution SAXS and CD measurements reveals an intimate relationship between secondary structure and morphology, and their evolution in time. For the first time, to our knowledge, the formation of nanotubes by the disruption of β-sheet structures has been observed. Interestingly, intense ultraviolet irradiation has been found to photo-degrade these weakly-coupled conformations in PNTs and trigger the reverse phase transition. Counter-ion condensation and affinity between Na^+ ions and carboxylate groups at glutamic acid moieties are likely a driving forcing leading to scrolling into

tubular structures and could be used in the future to control formation of peptide nanotubes.

This work was supported by FAPESP (No. 2014/03515-8 and 2013/12997-0) and EPSRC EP/L020599/1 to IWH.

Notes and references

[a] *Centro de Ciências Naturais e Humanas, Universidade Federal do ABC, Santo André 09210-580, Brazil. E-mail: ersilva@ufabc.edu.br*
[b] *Dept of Chemistry, University of Reading, Whiteknights Reading, Berkshire RG6 6AD, UK. E-mail: i.w.hamley@reading.ac.uk*
[c] *Dept of Applied Physics, Aalto University School of Science, P. O. Box 15100, FI- 00076, Finland*
[d] *Diamond Light Source Ltd, Harwell Science and Innovation campus, Didcot, Oxfordshire OX11 0DE, UK*

† Electronic Supplementary Information (ESI) available: [methods, fluorescence, CD and IR *spectra*, SAXS fitting, XRD, Cryo-TEM, calculations]. See DOI: 10.1039/b000000x/

‡ Footnotes should appear here. These might include comments relevant to but not central to the matter under discussion, limited experimental and spectral data, and crystallographic data.

1. I. W. Hamley, *Soft Matter*, 2011, **7**, 4122-4138.
2. S. G. Zhang, *Accounts Chem. Res.*, 2012, **45**, 2142-2150.
3. A. H. Fuhrhop and T. Y. Wang, *Chemical Reviews*, 2004, **104**, 2901-2937.
4. N. Nuraje, H. Y. Bai and K. Su, *Prog. Polym. Sci.*, 2013, **38**, 302-343.
5. H. Cui, M. J. Webber and S. I. Stupp, *Biopolymers*, 2010, **94**, 1-18.
6. A. Dehsorkhi, V. Castelletto and I. W. Hamley, *Journal of Peptide Science*, 2014, **20**, 453-467.
7. A. Aggeli, N. Boden and Z. Shuguang, eds., *Self-Assembling Peptide Systems in Biology, Medicine and Engineering* Springer Netherlands, 2001.
8. S. S. Santoso, S. Vauthey and S. G. Zhang, *Curr Opin Colloid In*, 2002, **7**, 262-266.
9. X. Zhao, F. Pan, H. Xu, M. Yaseen, H. Shan, C. A. E. Hauser, S. Zhang and J. R. Lu, *Chem. Soc. Rev.*, 2010, **39**, 3480-3498.
10. Z. Shen, T. Wang and M. Liu, *Chem Commun (Camb)*, 2014, **50**, 2096-2099.
11. P. Gao and M. Liu, *Langmuir*, 2006, **22**, 6727-6729.
12. C. Zhan, P. Gao and M. Liu, *Chem Commun (Camb)*, 2005, 462-464.
13. M. Kogiso, S. Ohnishi, K. Yase, M. Masuda and T. Shimizu, *Langmuir*, 1998, **14**, 4978-4986.
14. W. H. Landschulz, P. F. Johnson and S. L. Mcknight, *Science*, 1988, **240**, 1759-1764.
15. E. K. Oshea, R. Rutkowski and P. S. Kim, *Science*, 1989, **243**, 538-542.
16. I. W. Hamley, *Angew Chem Int Edit*, 2014, **53**, 6866-6881.
17. C. C. Decandio, E. R. Silva, I. W. Hamley, V. Castelletto, M. S. Liberato, V. X. Oliveira, Jr., C. L. Oliveira and W. A. Alves, *Langmuir*, 2015.
18. T. Y. Wang, J. A. Jiang, Y. Liu, Z. B. Li and M. H. Liu, *Langmuir*, 2010, **26**, 18694-18700.
19. L. Ziserman, H. Y. Lee, S. R. Raghavan, A. Mor and D. Danino, *J Am Chem Soc*, 2011, **133**, 2511-2517.
20. J. S. Pedersen, *Advances in Colloid and Interface Science*, 1997, **70**, 171-210.
21. G. Pabst, M. Rappolt, H. Amenitsch and P. Laggner, *Phys Rev E Stat Phys Plasmas Fluids Relat Interdiscip Topics*, 2000, **62**, 4000-4009.
22. T. E. Creighton, *Proteins : structures and molecular properties*, W.H. Freeman, New York, 2nd edn., 1993.
23. R. Schmid, A. M. Miah and V. N. Sapunov, *Phys Chem Chem Phys*, 2000, **2**, 97-102.
24. S. D. Moran and M. T. Zanni, *J Phys Chem Lett*, 2014, **5**, 1984-1993.
25. I. W. Hamley, *Angew Chem Int Ed Engl*, 2007, **46**, 8128-8147.
26. A. Barth, *Prog Biophys Mol Biol*, 2000, **74**, 141-173.
27. B. Nordén, A. Rodger, T. Dafforn and Royal Society of Chemistry (Great Britain), *Linear dichroism and circular dichroism : a textbook on polarized-light spectroscopy*, Royal Society of Chemistry, Cambridge, 2010.
28. N. Sreerama and R. W. Woody, *Protein Sci*, 2003, **12**, 384-388.
29. V. Castelletto, I. W. Hamley, C. Cenker, U. Olsson, J. Adamcik, R. Mezzenga, J. F. Miravet, B. Escuder and F. Rodriguez-Llansola, *J Phys Chem B*, 2011, **115**, 2107-2116.
30. D. I. Pattison, A. S. Rahmanto and M. J. Davies, *Photochemical & Photobiological Sciences*, 2012, **11**, 38-53.
31. H. Cui, E. T. Pashuck, Y. S. Velichko, S. J. Weigand, A. G. Cheetham, C. J. Newcomb and S. I. Stupp, *Science*, 2010, **327**, 555-559.